AIAA JOURNAL
Vol. 44, No. 3, March 2006

Modeling and Application of Eddy Current Damper for Suppression of Membrane Vibrations

Henry A. Sodano*
Michigan Technological University, Houghton, Michigan 49931-1295
Jae-Sung Bae†
Korea Institute of Energy Research, Daejeon 305-343, Republic of Korea
Daniel J. Inman‡
Virginia Polytechnic Institute and State University, Blacksburg, Virginia 24061-0261
and
W. Keith Belvin§
NASA Langley Research Center, Hampton, Virginia 23681-0001

Inflatable space-based structures have become increasingly popular over the past three decades due to their minimal deployed mass and launch volume. To facilitate packaging of the satellite in the shuttle bay, the optical or antenna surface is in many cases a thin-film membrane. Additionally, because the structure holding the membrane is a lightweight and flexible inflated device, the membrane is subjected to a variety of dynamic loadings. For the satellite to perform optimally, the membrane structure must be free of vibration. However, due to the extreme flexibility of the membrane, the choice of applicable sensing and actuation methods to suppress the vibration is limited. The present study investigates the use of an eddy current damper to passively suppress the vibration of a thin membrane. Eddy currents are induced when a nonmagnetic conductive material is subjected to a time-changing magnetic flux. As the eddy currents circulate inside the conductor they are dissipated, causing energy to be removed from the system and thus allowing the system to function as a type of viscous damper. Using this concept, the ability to generate sufficient damping forces in the extremely thin-film membranes used in space is studied. First, a theoretical model of the interaction between the eddy current damper and the membrane is developed. The model is then validated through experiments carried out at both ambient and vacuum pressures. The results show that the model can accurately predict the damping of the first mode as the distance between the magnet and membrane is varied. Furthermore, the results of the experiments performed on the membrane at vacuum conditions show the functionality of the damping mechanism in space and indicate damping levels as high as 30% of critical at ambient pressure and 25% of critical at vacuum pressure.

Nomenclature

A	=	half the conductor's length
$\boldsymbol{B}$	=	magnetic flux density
b	=	radius of the circular magnet
$\boldsymbol{C}$	=	damping matrix
$\boldsymbol{C}_b$	=	damping matrix of beam
c_e	=	eddy current damping coefficient
E	=	modulus of elasticity
F	=	concentrated forces
$\boldsymbol{F}$	=	damping force
f	=	distributed forces
$\boldsymbol{J}$	=	eddy current density
$\boldsymbol{K}$	=	stiffness matrix
L	=	length of magnet
L_m	=	length of membrane
l_g	=	gap length between magnet and conductor
$\boldsymbol{M}$	=	mass matrix
M_0	=	magnetization
P	=	axial load
Q	=	external forces
$r(t)$	=	temporal coordinate
r_c	=	equivalent radius of the conductor
T	=	kinetic energy
t	=	time
U	=	potential energy
V	=	volume
$\boldsymbol{v}$	=	velocity of conductor
v_z	=	velocity of beam in z direction
w	=	displacement
δ	=	thickness of conductor
ζ	=	damping ratio
μ_0	=	permeability of free space
$\rho(x)$	=	area density
σ	=	conductivity
$\phi(x)$	=	assumed mode shapes
ϕ_e	=	magnitude of mode shape at location of eddy current damper

Received 30 August 2004; revision received 18 August 2005; accepted for publication 13 October 2005.

*Assistant Professor and NASA Fellow, Department of Mechanical Engineering–Engineering Mechanics, 815 R.L. Smith ME-EM Building, 1400 Townsend Drive; hsodano@mtu.edu. Member AIAA.

†Senior Researcher, Wind Power/Fluid Machinery Research Center, Department of New and Renewable Energy Research; jsbae@kier.re.kr. Member AIAA.

‡G.R. Goodson Professor and Director for Center for Intelligent Material Systems and Structures, Department of Mechanical Engineering, 310 Durham Hall; dinman@vt.edu. Fellow AIAA.

§Aerospace Engineer, Mail Stop 230, Structure Division, 4B West Taylor Street; w.k.belvin@larc.gov. Member AIAA.

Introduction

INFLATABLE structures show significant promise for future space applications due to their low mass and volume in the launch configuration. Although many different satellite and solar sail designs have been proposed, to facilitate the packaging of the inflated device in its launch configuration, most structures utilize a

thin-film membrane as the optical or antenna surface. Once the inflated structure is deployed in space, the structure is subject to vibrations induced mechanically by guidance systems and space debris as well as to thermally induced vibrations from variable amounts of direct sunlight. For optimal performance of the satellite, it is crucial that the vibration of the membrane be quickly suppressed. However, due to the extremely flexible nature of the membrane structure, few actuation methods exist that avoid local deformation and surface aberrations.

The actuation method most commonly investigated with membrane structures is the electrostatic actuator, which provides noncontact excitation forces to the structure. An early study of the use of electrostatic actuators for control of an optical membrane was performed in 1977 by Grosso and Yellin.[1] The authors used an array of 53 hexagonal electrostatic actuators located 50–100 μm away from the membrane surface and could generate a typical deflection of one-half wave with less than 100 V applied and a deflection of several waves when numerous actuators were used. Their study also presented the basic design equations for the actuated membrane and showed its accuracy through experiments. A later study was performed by Claflin and Bareket,[2] who investigated the ability to use electrostatic actuators to generate shape functions on the surface of the membrane mirror. Their study investigates an approximate analytic solution of Poisson's equation that allows determination of the influence functions for a circular electrostatic mirror and thus the optimal control voltage for each actuator. The process was demonstrated on a circular membrane mirror developed by Merkle et al.[3] that utilized 109 electrostatic actuators and was shown to be capable of reproducing Zernike polynomials up to degree 6 with good accuracy.

Although electrostatic actuators have received a vast amount of research, other actuation methods have been studied. Divoux et al.[4] studied the use of microcoils and a membrane coated with a magnetic material. When a current is applied to the coil, a magnetic field is generated and thus a noncontact force is applied to the membrane surface. Nelson and Main[5] bonded a polyvinylidene fluoride piezoelectric patch to the surface of a membrane that could be excited by applying a bias voltage to one side and firing an electron gun at the other surface. Using this method the strain of the piezoelectric could be controlled and discrete areas of the patch could be excited. Wagner[6] constructed a membrane mirror with polyvinylidene fluoride material bonded to the surface. Four mirrors with various electrode patterns were constructed and tested to determine the effectiveness of each. It was shown that by varying the excitation voltage a maximum deflection of 32 μm could be obtained. Solter et al.[7] used a macrofiber composite actuator and piezoelectric stack to apply boundary control to suppression of a membrane antenna's vibration. Using the stack actuator the in-plane tension was controlled and with the macrofiber composite, the out-of-plane motion was controlled. From one of 12 tensioning cables the excitation force was applied and the system was shown to reduce the magnitude of vibration above 15 Hz.

Another method of inducing noncontact forces that has not been investigated previously for use with membrane structures is eddy currents. Eddy currents are generated when a nonmagnetic conductive material is subjected to a time-varying magnetic flux. Time-varying magnetic flux can be induced on the conductive material by holding the magnetic source at a constant position or intensity and moving the conductor relative to the magnetic source or by holding the position of the conductor constant and varying the magnetic source's position or intensity. Eddy currents that are generated in the conductive material circulate so that a magnetic field of the same polarity as the applied magnetic field is generated, thus causing a repulsive force between the magnet and conductor. However, due to the electrical resistance of the conductive material, the eddy currents will dissipate into heat at the rate of I^2R and the force will disappear. In the case of a dynamic system, the position of the conductor is continually changing with respect to a fixed permanent magnet, therefore inducing an electromotive force (emf) and allowing the eddy currents to be regenerated. The result of the generation and dissipation of the eddy currents is that an amount of energy proportional to the velocity of the conductor is removed from the dynamic system, thus resulting in a viscous damping mechanism.

The ability to use eddy currents for the purpose of applying damping to dynamic systems has been known for a considerable amount of time, with the majority of the work performed on magnetic braking[8–11] and lateral vibration control of rotating machinery[12,13]; both topics have been thoroughly investigated. Although the theory and applications of rotary magnetic braking systems have been well documented, there are many more applications of eddy current dampers. Karnopp[14] introduced the idea that a linear electrodynamic motor consisting of coils of copper wire and permanent magnets could be used as an electromechanical damper for vehicle suspension systems. He showed that his actuator could be much smaller and lighter than conventional actuators although still providing effective damping in the frequency range typically encountered by road vehicle suspension systems. Schmid and Varga[15] studied a vibration-reducing system with eddy current dampers (ECDs) for high-resolution and nanotechnology devices such as a scanning tunneling microscope. Kobayashi and Aida[16] explored the use of a Houde damper (a type of damped vibration absorber) using an ECD as the energy dissipation mechanism. The ECD consisted of a conducting plate moving between two permanent magnets. The study found that the Houde damper could increase the damping ratio by 2% and suppress the displacement of a pipe by a factor of 8–10. Kienholtz et al.[17] investigated the use of a magnetic tuned-mass damper for vibration suppression of a spacecraft solar array and a magnetically damped isolation mount for the payload inside of a space shuttle. The magnetic tuned-mass damper system targeted two modes of the solar array (first torsion at 0.153 Hz and first out-of-plane bending at 0.222 Hz) and increased the damping by 30 and 28 dB, respectively, whereas the higher-frequency untargeted modes at 0.4–0.8 Hz were damped in the range of 11–16 dB.

More recently, Kwak et al.[18] developed an ECD for the transverse vibration of a cantilever beam. The damper was constructed with a copper conducting plate and flexible magnetic linkage attached to the tip of the beam. When the beam is set into vibration the flexible linkage swings along the copper plate, causing the vibrations to damp out. The authors constructed the damper and their experimental results showed that the eddy current damper can be an effective device for vibration suppression. Later, Bae et al.[19] modified and developed the theoretical model of the eddy current damper constructed by Kwak et al.[18] Using this new model, the authors investigated the damping characteristics of the ECD and simulated the vibration suppression capabilities of a cantilever beam with an attached ECD numerically.

When eddy currents are used the typical method of inducing an emf in the conductive metal is to place the metal directly between two oppositely poled magnets with the metal moving perpendicular to the magnets' poling axis. A schematic of this process is shown in Fig. 1 and has been studied in Refs. 8–19. This configuration

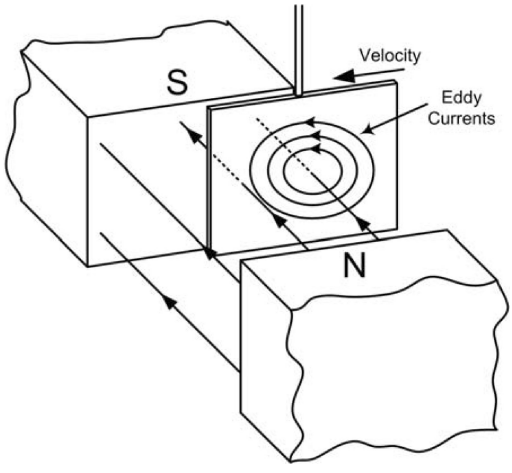

Fig. 1 Schematic of conductive material passing through a magnetic field and generation of eddy currents.

is optimal because of the concentrated magnetic field between the two magnets. Although this configuration is effective for magnetic braking, in certain applications it is not possible, for example, the transverse vibrations present in many dynamic systems. The studies that have used this configuration to damp the transverse vibration of a structure have produced cumbersome and ineffective dampers. Therefore, Sodano et al.[20] proposed and developed a theoretical model of one such system in which the transverse vibrations of a cantilever beam were damped by a permanent magnet fixed to a location perpendicular to the beam's motion and the magnet's radial flux was used to generate the damping force. It was shown through experiments that the theoretical model very accurately estimated the damping when the magnet was more than 5 mm from the beam, but was less accurate for smaller gaps. This occurs due to the conductor's size being only slightly greater than that of the magnet, causing the flux outside the conductor to be significant up to 5 mm for the geometry used. To account for this problem Sodano et al.[21] utilized the image method, which allows the electrical boundary conditions of the conductor to be satisfied. The authors show that using this technique the accuracy of the mathematical model can be greatly increased. Furthermore, Sodano et al.[21] develop an improved concept for an ECD that significantly increases the damping force applied to the structure. The ECDs developed in Refs. 20 and 21 provide many advantages over other commonly used damping techniques, making them ideal for the flexible nature of the membrane structure. The ECD does not contact the structure, thus allowing the damper to be easily incorporated into the system. Furthermore, because the damper is of noncontact nature, the structural properties are not affected by its addition to the system and the force is distributed, therefore avoiding local deformation of the membrane. Additionally, the ECD is capable of generating significant damping forces; for instance, the damper used by Sodano et al.[21] was able to achieve critical damping of a cantilever beam. For these reasons the ECD would be an ideal choice for applying significant damping to the membrane.

In the present study, the eddy current damper concept developed by Sodano et al.[20] will be utilized to attenuate the vibration of a membrane strip. A model to predict the dynamic interaction between the membrane and the damper will be developed. The accuracy of the model will be shown through experiments performed in ambient and vacuum conditions. The damper will be demonstrated to be effective in vacuum conditions, which is a necessary property of any system intended for space. Additionally, the model of the system will be shown to predict the system damping for both vacuum and ambient conditions. The results presented in this paper will demonstrate the effectiveness of noncontact ECDs for use with thin film membranes.

Eddy Current Damper Model

The configuration of the dynamic system used in this study is shown in Fig. 2, and consists of a slender membrane under tension that is simply supported at both boundaries. The damping mechanism consists of a conductive copper foil placed at the center of the membrane and a permanent magnet located a small distance from the conductor. Figure 3 shows a conducting sheet of thickness δ and conductivity σ moving with velocity $\boldsymbol{v}$ in the air gap l_g of a circular magnet. The axes of Fig. 3 are defined in Cartesian coordinates. The x and y coordinates represent the radial directions extending out parallel to the face of the permanent magnet and the z coordinate represents the poling axis of the magnet. Because of the permanent magnet, a magnetic field is generated in the vertical (z) and horizontal or radial (y or R) axes. For the dynamic system considered in this research, the membrane moves perpendicular to the face on the permanent magnet or in the vertical (z) direction, thus allowing only the radial magnetic flux to generate eddy currents. As shown in Fig. 3, the eddy currents will circulate in the x–y plane, causing a magnetic field to be generated in the vertical (z) direction. The magnetic field generated by the eddy currents will fluctuate in polarity depending on the direction the membrane is traveling, thus causing the damping force to be induced on the membrane.

Because of the symmetry of the circular permanent magnet, the surface charges are ignored, allowing the eddy current density $\boldsymbol{J}$ induced in the conducting sheet moving in the vertical direction to be written as

$$\boldsymbol{J} = \sigma(\boldsymbol{v} \times \boldsymbol{B}) \tag{1}$$

where the $\boldsymbol{v} \times \boldsymbol{B}$ term is the cross product of the velocity $\boldsymbol{v}$ of the conductor and the magnetic flux density $\boldsymbol{B}$ defining the emf driving the eddy currents $\boldsymbol{J}$. The velocity and magnetic flux can be written

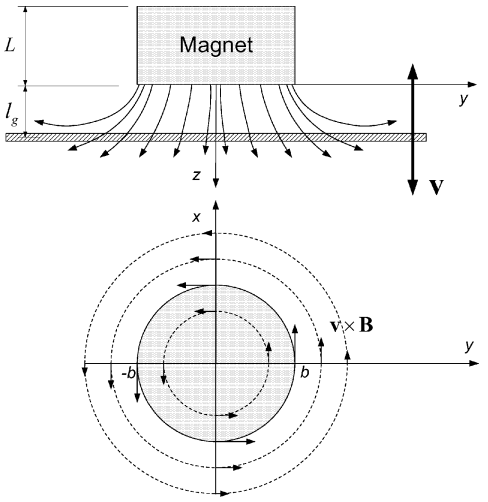

Fig. 3 Magnetic field and the eddy currents induced in the cantilever beam.

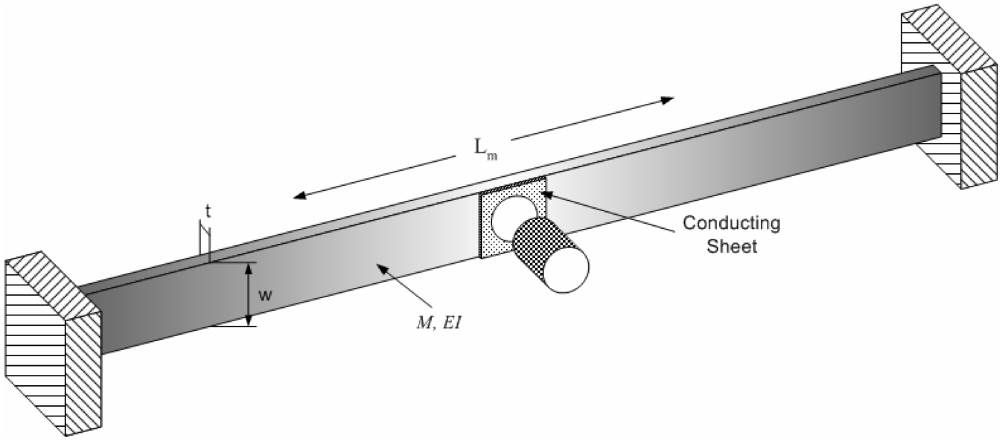

Fig. 2 Configuration of the membrane strip, conductor, and magnet.

as follows:

$$\boldsymbol{v} = 0\boldsymbol{i} + 0\boldsymbol{j} + v_z\boldsymbol{k} \tag{2}$$

$$\boldsymbol{B} = B_x\boldsymbol{i} + B_y\boldsymbol{j} + B_z\boldsymbol{k} \tag{3}$$

where the velocity of the conductor is only in the z direction. After substitution of Eqs. (2) and (3) into Eq. (1), the eddy current density is defined by

$$\boldsymbol{J} = \sigma(\boldsymbol{v} \times \boldsymbol{B}) = \sigma v_z(-B_y\boldsymbol{i} + B_x\boldsymbol{j}) \tag{4}$$

This equation confirms that the magnetic flux in the z direction has no effect on the induced eddy currents and that the induced currents are solely dependent on the x and y components of the magnetic flux or the flux tangential to the face of the conducting sheet.

To determine the eddy current density in the conducting sheet, the magnetic flux of the permanent magnet must be found. For the case of a cylindrical permanent magnet, the equation defining the flux density has been derived by Sodano et al.[21]; thus the only resulting equations for the magnetic flux density of the permanent magnet will be provided. The radial and transverse magnetic flux density due to the circular magnet of length L are written as

$$B_y(y, z) = \frac{\mu_0 M_0 b}{4\pi} \int_{-L}^{0} (z - z')I_1(b, y, z - z')\,\mathrm{d}z' \tag{5}$$

$$B_z(y, z) = \frac{\mu_0 M_0 b}{4\pi} \int_{-L}^{0} I_2(b, y, z - z')\,\mathrm{d}z' \tag{6}$$

where z' is the distance in the z direction from the center of a magnetized infinitesimal strip, b is the radius of the permanent magnet, M_0 is the magnetization per unit length, and I_1 and I_2 include the elliptic integrals and are shown in the Appendix. As indicated in Fig. 2, the magnetic field distributions in Eqs. (5) and (6) are symmetric about the z axis and because of the complexity of the integrals, they must be solved numerically.

Before solving for the damping force, the image method is applied to the eddy current density to satisfy the electrical boundary conditions. The image method works by taking a mirror image of the predicted eddy current density, rotating that image about the edge of the conductor, and then taking the difference of the two.[21] The effect of this is to force the eddy current density at the boundary of the conductor to be zero. A schematic of how the image method functions is shown in Fig. 4. The net eddy current density can then be written as follows:

$$\boldsymbol{J}' = \left(J_y^{(1)} - J_y^{(2)}\right) \tag{7}$$

where y is the radial direction and the imaginary eddy current density $J_y^{(2)}$ is written as

$$J_y^{(2)}(y) = J_y^{(1)}(2A - y) \tag{8}$$

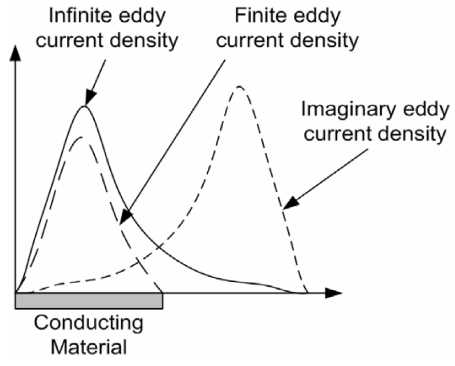

Fig. 4 Schematic demonstrating the effect of the imaginary eddy currents.

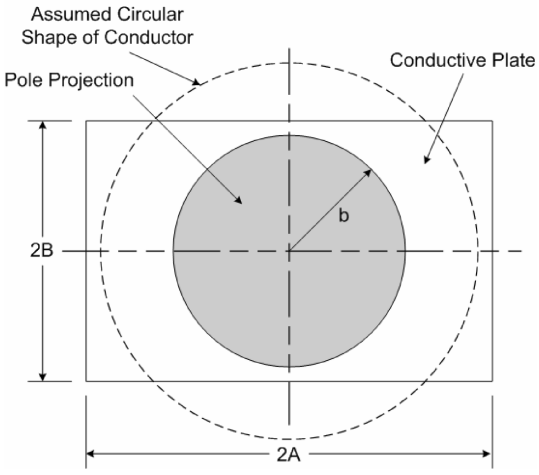

Fig. 5 Schematic showing the variables associated with the conducting plate.

where A is the half the length of the conductor, as shown in Fig. 5. Only the y component of the eddy current density is used in the equation because of the eddy current density being symmetric around the conductor, which is assumed to be of circular geometry with the surface area the same as the rectangular conductor, as shown in Fig. 5. The conductor is assumed to be circular to simplify the integration of Eqs. (5) and (6) as well as the integration of the damping force, which will now be defined.

Because the velocity of the conducting sheet is in the z direction, the magnetic flux density B_z does not contribute to the damping force, as shown in Eq. (4). Using Eqs. (4), (5), (7), and (8), the damping force between the permanent magnet and the eddy current is defined by

$$\begin{aligned}\boldsymbol{F} &= \int_V \boldsymbol{J}' \times \boldsymbol{B}\,\mathrm{d}V \\ &= -\boldsymbol{k}\sigma\delta v_z\left[\int_0^{2\pi}\int_0^{r_c} yB_y^2(y, l_g)\,\mathrm{d}y\,\mathrm{d}\phi\right. \\ &\quad \left. - \int_0^{2\pi}\int_0^{r_c} yB_y^2(2A - y, l_g)\,\mathrm{d}y\,\mathrm{d}\phi\right] \\ &= -\boldsymbol{k}2\pi\sigma\delta v_z\left[\int_0^{r_c} yB_y^2(y, l_g)\,\mathrm{d}y - \int_0^{r_c} yB_y^2(2A - y, l_g)\,\mathrm{d}y\right]\end{aligned} \tag{9}$$

where as before δ and v are the thickness and the vertical velocity of the conducting sheet, respectively, as shown in Fig. 3. The analytic integration of Eq. (9) is too difficult and the equation must therefore be solved using numerical integration techniques.

After the force generated by the eddy currents is determined, the membrane must be modeled and the damping force integrated into the model, so that the dynamic response can be predicted. The membrane used for this research effort was chosen to resemble a beam rather than a two-dimensional membrane, thus allowing dynamic testing to be more easily performed at vacuum pressure. Because the membrane is extremely flexible, in both excitation and sensing methods are very limited. By using a one-dimensional membrane, experimentally identifying bending modes and correlating them with the model are greatly simplified. Furthermore, the question is not whether the passive eddy current damping techniques will work on a two-dimensional membrane but rather whether they will generate sufficient damping forces on a very thin structure. The damping force that can be generated by a very thin structure is questionable, because from Eq. (7), it has been shown that the damping force is directly proportional to the thickness of the conducting

material and thus the thin materials used for membranes may not generate forces sufficient to damp the structure.

Although the membrane used in this research is a one-dimensional structure and could be modeled as a string, the copper conductor bonded to the membrane material is not devoid of stiffness. Therefore a beam model must be used to allow the stiffness of the copper patch to be included in the model. The structure can be modeled as an Euler–Bernoulli beam subjected to an axial load. The equation of motion for a beam under an axial load was formulated by Shaker[22] in 1975 as

$$\frac{\partial^4 w(x,t)}{\partial x^4} + \frac{P}{EI(x)}\frac{\partial^2 w(x,t)}{\partial x^2} + \frac{\rho(x)}{EI(x)}\frac{\partial^2 w(x,t)}{\partial t^2} = 0 \quad (10)$$

where $w(x,t)$ is the transverse deflection of the beam, $\rho(x)$ is the mass per unit length, and EI is the beading stiffness of the beam in two quantities, one for the membrane and one for the foil area. From the equation of motion the kinetic energy and potential energy can be written as

$$T = \frac{1}{2}\int_0^{L_m} \rho(x)\left[\frac{\partial w(x,t)}{\partial t}\right]^2 \mathrm{d}x \quad (11)$$

$$U = \frac{1}{2}\int_0^{L_m} \left\{ EI(x)\left[\frac{\partial^2 w(x,t)}{\partial x^2}\right]^2 + P\left[\frac{\partial w(x,t)}{\partial x}\right]^2 \right\} \mathrm{d}x \quad (12)$$

where L_m is the length of the beam. Next the assumed modes method is used to write the displacement of the beam as the summation of the beam's mode shapes and a temporal coordinate:

$$w(x,t) = \sum_{i=1}^{n} \phi_i(x) r_i(t) \quad (13)$$

where $\phi_i(x)$ is the ith eigenfunction and n is the number of modes to be considered. Using this assumption the temporal coordinate can be factored, allowing the kinetic energy and potential energy to be simplified to the mass and stiffness matrix as

$$\boldsymbol{K} = \int_0^{L_m} EI(x)\left(\frac{\mathrm{d}^2\bar{\phi}(x)}{\mathrm{d}x^2}\right)^T \frac{\mathrm{d}^2\bar{\phi}(x)}{\mathrm{d}x^2}\,\mathrm{d}x + \int_0^{L_m} P\left(\frac{\mathrm{d}\bar{\phi}(x)}{\mathrm{d}x}\right)^T \frac{\mathrm{d}\bar{\phi}(x)}{\mathrm{d}x}\,\mathrm{d}x \quad (14)$$

$$\boldsymbol{M} = \int_0^{L_m} m(x)\phi^T(x)\phi(x)\,\mathrm{d}x \quad (15)$$

where $\boldsymbol{M}$ and $\boldsymbol{K}$ are the mass and stiffness matrices, respectively. The external work can now be written as

$$\bar{Q}(t) = \int_0^{L_m} f(x,t)\bar{\phi}(x)\,\mathrm{d}x + \sum_{j=1}^{m} F_j(t)\bar{\phi}(x_j) \quad (16)$$

where $\bar{Q}(t)$ is the vector of external forces, $f(x,t)$ is a distributed force, F_j is the jth concentrated force, and m is the number of concentrated forces. Now the damping matrix can be defined as

$$\boldsymbol{C} = \left[\boldsymbol{C}_b + \phi^T c_e \phi\right] \quad (17)$$

where $\boldsymbol{C}_b$ and c_e are defined by

$$\boldsymbol{C}_b = 2\zeta\sqrt{\mathrm{diag}(\boldsymbol{KM})} \quad (18)$$

$$c_e = F/v_z \quad (19)$$

where ζ is the structural damping ratio of the membrane determined through experimental testing, F is the eddy current damping force in the z direction determined in Eq. (9), and v is the velocity of the beam. The product of the mass and stiffness is reduced to a diagonal matrix because the off-diagonal terms are negligible and the computation can be performed more easily. The equation of motion can now be written in a recognizable form as

$$\boldsymbol{M}\underline{\ddot{r}}(t) + \boldsymbol{C}\underline{\dot{r}}(t) + \boldsymbol{K}\underline{r}(t) = \underline{\phi}(x_i)^T f_i(t) \quad (20)$$

Equation (20) now describes the dynamics of the slender membrane subjected to an axial tension with the damping force due to the eddy currents included.

Experimental Setup

To validate the accuracy of the theoretical model, experiments were performed on a slender 12.7-μm-thick Mylar membrane tensioned between two simply supported edges. Because the Mylar material is not conductive, a patch of 35.6-μm-thick 3M 1181 copper foil tape was bonded to the membrane at its center. The dimensions and placement of the membrane and copper conductor are provided in Fig. 6. Other relevant properties of the Mylar membrane, copper conductor, and magnet are provided in Table 1. The copper conductor used was thin and ductile enough not to interfere with the flexibility of the membrane material; however, the effects of the copper patch had to be included in the model to maintain its accuracy.

The goals of the experiments performed in this study are to identify the damping ratio and frequency response of the slender membrane subjected to an axial load when at vacuum and ambient pressure. However, experimentally testing a membrane structure is very difficult because of limited choice of sensing and actuation methods, wrinkling, modal coupling, and sensitivity to both boundary conditions and air currents. The boundary conditions of the membrane were chosen to be pinned in order to maintain constant eigenfunctions as axial tension is applied.[22] The pinned boundary conditions were constructed by clamping the edge of the membrane strip between two 6.35-mm-diam steel rods, similar to the clamps used by Hall et al.[23] The axial load was applied to the membrane by attaching one of the pinned boundary conditions to a Velmex unislide lead screw, whereas the other pinned boundary condition was fixed to a

Table 1 Physical properties of the beam, conductor, and magnet

Property	Value
Young's modulus of Mylar membrane	4.7 GPa
Density of Mylar membrane	1390 kg/m^3
Young's modulus of copper conductor	131×10^7
Density of copper conductor	8910 kg/m^3
Conductivity of copper conductor	1.052×10^7
Permanent magnet composition	NdFeB 45
Residual magnetic flux of magnet	1.35 kG

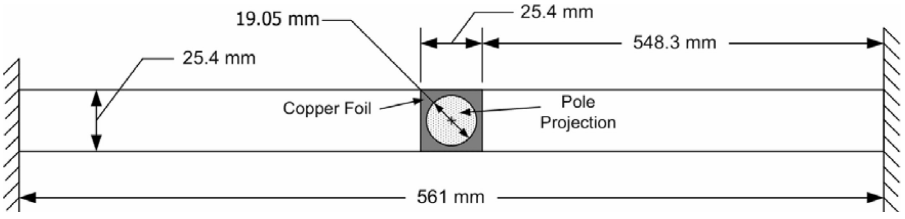

Fig. 6 Dimensions of membrane strip and location of copper conductor.

Transducer Techniques MLP-75 load cell that measured the force applied to the membrane by the lead screw, as shown in Fig. 7. By monitoring the load cell reading and adjusting the lead screw, the tension in the membrane could be accurately set. Because of the very high flexibility of the membrane, both sensing and actuation techniques must be carefully chosen. After several actuation schemes were tried, it was determined that the best method would be to attach the entire test fixture to a shaker and let the inertia of the membrane excite itself, as shown in Fig. 7. Sensing was performed using a Polytec laser vibrometer because it did not contact the structure during measurements. The last portion of the experimental setup is the positioning mechanism for the permanent magnet. To allow the magnet's position to be accurately varied, the magnet was bonded to a wooden block that was then fixed to a Velmex lead screw, as shown in Fig. 7. The magnet was fixed to a wooden block rather than a metal block to reduce interference with the magnetic flux.

Experiments were performed both at ambient and at vacuum pressure to determine how the performance of the eddy current damper varied and if it would be functional in space. During ambient testing the membrane was simply excited in a laboratory environment, but for vacuum testing the entire test setup was placed in a Tenahy 2-m vacuum chamber as shown in Fig. 8. During testing the chamber was reduced to 0 torr before experiments were performed. The only change that needed to be made to the test setup when it was placed in the vacuum chamber was to the wooded block the magnet was bonded to, which was required to be switched to a high-density plastic. This was required because as the air was removed from the chamber the moisture in the wooden block was also removed, causing the block to shrink. The vacuum chamber had a glass window that allowed the laser vibrometer to be used to measure the membrane's vibration. It was found through experiments that the glass window did not affect the quality of the measured data, but rather, the data's quality was actually improved due to isolation from air currents in the chamber.

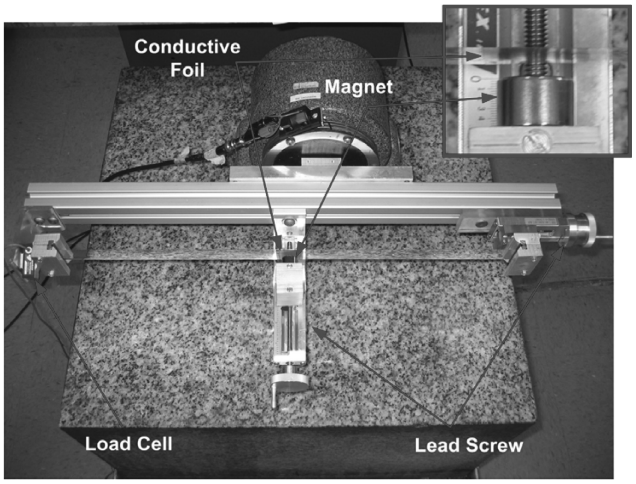

Fig. 7 Experimental setup used to determine the damping effect of the permanent magnet as the distance from the conductor is varied.

Results and Discussion

The scope of this research is to show the ability of the eddy current damping system developed by Sodano et al.[20] to add significant damping to a thin membrane structure and develop an accurate model of the damping mechanism's interaction with the membrane. The ability of the eddy current damping system to add damping into the structure is shown by measuring the frequency response before and after placement of the magnet. Figure 9 shows the frequency response of the membrane when the ECD is not present in the system and for the case in which the magnet is located at a distance of 1 mm from the membrane's surface. To help identify the modes shown in Fig. 9, the frequencies are labeled B1 for first bending mode, B2 for second bending, T1 for first torsional, and so on. Additionally, Table 2 provides the frequency of each of the first four bending modes and the first three torsional modes both when the membrane is at ambient and when it is at vacuum pressure. It can be seen from Fig. 9 that the damper provides significant damping to the membrane, reducing the magnitude of the first bending mode by 13.7 dB and the third bending mode by 5.2 dB. The second and fourth bending modes do not show any additional damping because the magnet is located at the center of the membrane strip, which is a nodal point for these modes.

Table 2 Bending and torsional natural frequencies of the membrane with a tension of 8.9 N both under vacuum and at ambient pressure

Mode shape	Ambient pressure, Hz	Vacuum pressure, Hz
First bending, B1	62	71.7
First torsional, T1	88.5	157
Second bending, B2	154	194.5
Second torsion, T2	178	212
Third bending, B3	205.8	242.5
Third torsion, T3	249	326
Fourth bending, B4	307.5	379.7

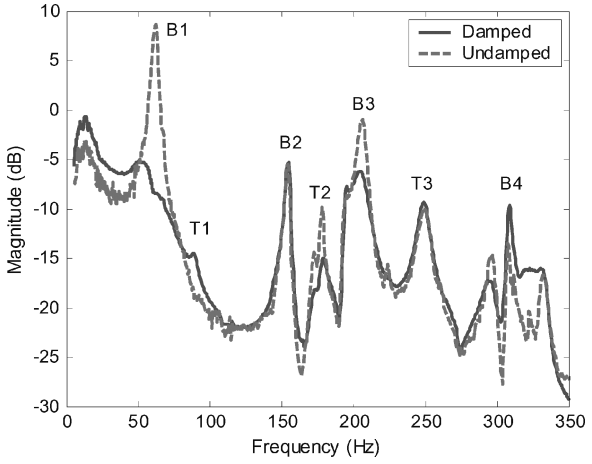

Fig. 9 Measured frequency response without magnet and with magnet a distance of 1 mm from membrane.

Fig. 8 Experimental setup in the vacuum chamber.

During tests on the membrane under vacuum conditions it was found that the eddy current damping system reduces the magnitude of the response better than at ambient conditions. The frequency response of the membrane when the damping mechanism was not present and when the magnet was located 1 mm from the surface of the membrane is shown in Fig. 10. From the figure it can be seen that the magnitude of the first bending mode is reduced by 31.06 dB and that of the third bending mode by 15.62 dB. As with the ambient tests, the second and fourth bending frequencies are not damped by the magnet because it is located at a nodal point of the modes.

Although the damper performs well under vacuum, the dynamic response of the membrane changes fairly significantly when subjected to vacuum pressure. The change in the frequency response of the membrane between ambient and vacuum pressure are compared in Fig. 11, and the shift in natural frequency for each mode can be seen in Table 2. The change in dynamic response can be attributed to the hygroscopic effects of the Mylar material and the decreased damping from the removal of air. The hygroscopic effects occur due to the moisture in the Mylar material being expelled as the pressure drops to vacuum. This causes the polymer material to shrink and the tension applied to the membrane to increase. The increase in tension could be measured using the load cell, but the effect on other material properties, such the elastic modulus and density, could not be measured and, therefore, could not be included in the theoretical model of the system. For more information on the hygroscopic effect of polymers at vacuum pressure; see Bales et al.[24] The amount of damping present in the system was determined by applying the unified polynomial matrix approach to the frequency response data. Using the unified polynomial matrix approach method, the damping ratio of the membrane system was determined for the magnet being placed at various distances from the membrane surface under both ambient and vacuum conditions. The resulting damping ratio of the membrane for each case is shown in Fig. 12. As can be seen in the figure, the damping ratio maintains almost a constant offset of approximately 0.025 over the tested range. The decrease in damping when the membrane is placed in a vacuum can be attributed to lack of air damping which can make a significant difference in lightweight structures such as membranes.

After the performance of the eddy current damper was tested under both ambient and vacuum conditions the accuracy of the model could be validated against the measured data. Using the model of the eddy current damping system that has been developed in this manuscript, the frequency response of the membrane could be predicted as a function of the gap between the magnet and the membrane surface. The predicted and measured damping ratios for the membrane at ambient pressure for various gaps between the magnet and the membrane surface are shown in Fig. 13. It can be seen from the figure that the model accurately predicts the damping ratio over the entire range of gap lengths.

Next, the accuracy of the model was tested for the case of a membrane placed under vacuum. However, due to changes in material

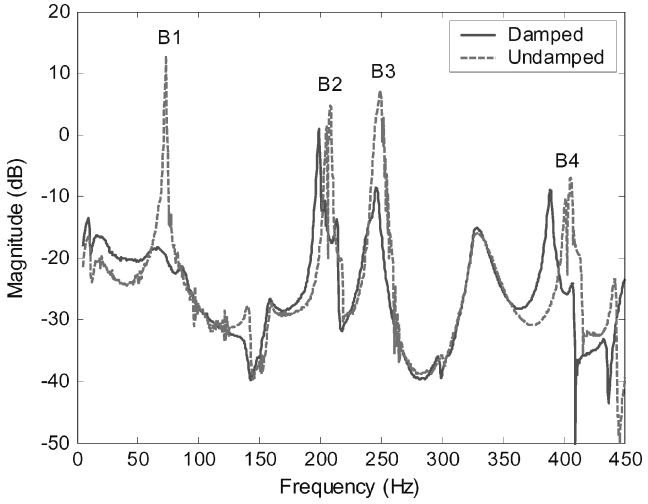

Fig. 10 Measured frequency response without magnet and with magnet a distance of 1 mm from membrane under vacuum and at an axial load of 8.9 N.

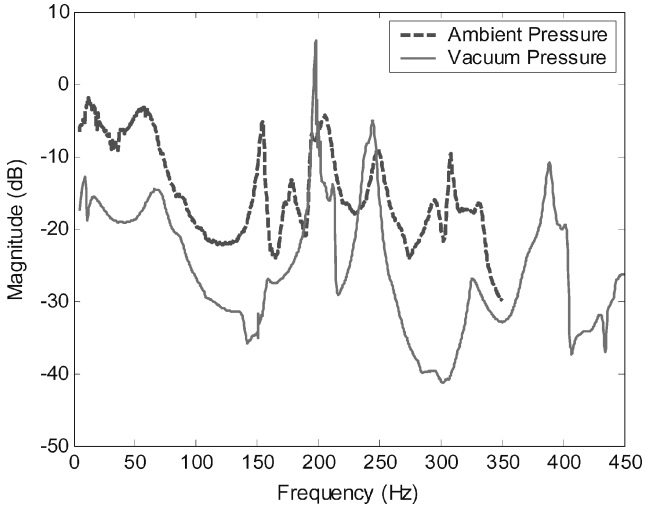

Fig. 11 Measured frequency response at ambient and vacuum pressure with magnet gap of 2 mm and an axial load of 8.9 N.

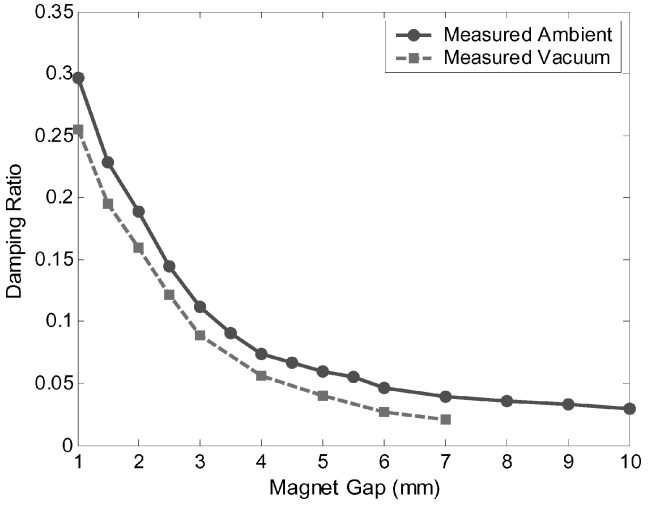

Fig. 12 Measured damping ratio of membrane at both ambient and vacuum pressure with an axial load of 8.9 N.

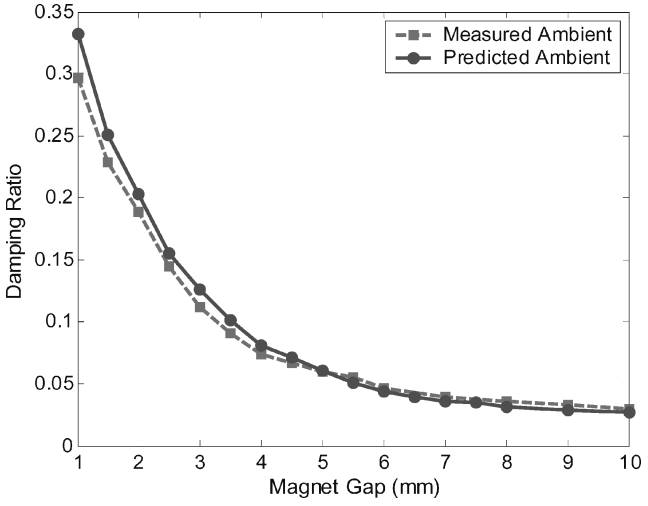

Fig. 13 Measured and predicted damping ratios of membrane at ambient pressure with an axial load of 8.9 N.

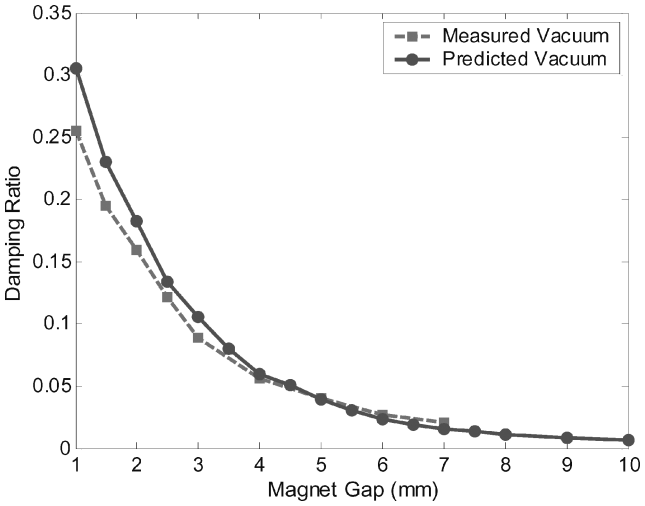

Fig. 14 Measured and predicted damping ratio of membrane under vacuum with an axial load of 8.9 N.

size and properties resulting from the hygroscopic effects of the Mylar membrane, the frequency response could not be accurately modeled. As previously mentioned, when the pressure around the Mylar drops to vacuum, the water content of the polymer is expelled, thus causing the material volume and properties to change. The only change in the material that could be measured was reduction of length, which was measured as an increase in axial load using the load cell. Because the other properties could not be found, the model could not be used to predict the frequency response. However, the predicted damping ratio of the first mode under vacuum maintained accuracy, as shown in Fig. 14.

The damping mechanism detailed in the paper has several advantages over other methods of applying damping to the membrane. Because the intended use of this technology is to damp the vibrations of optical or antenna membranes, the surface must remain flat, which limits the types of damping devices that can be used. This point brings up one of the major advantages of this type of damping mechanism: the damper is noncontact and therefore does not cause inconsistencies on the membrane surface that would arise from bonding. The damper also applies a distributed force on the surface of the membrane, which is necessary to achieve global damping and avoid local deformation. Furthermore, because the damper is noncontact, it does not change the dynamic response of the system, which can be seen in Figs. 9 and 10. Another advantage of this type of damper is that it is extremely easy to install and only modifies the system damping. Additionally, magnetic dampers do not require any maintenance to stay functional, which is a very important trait of any space system. For these reasons, magnetic damping mechanisms are an excellent choice for use in space.

Conclusions

The interest in developing inflatable space devices has blossomed in the past few decades because of their low volume and mass in launch configuration. Once in space, these structures are deployed and inflated and they become extremely large. Because the structure is flexible and packaged in the space shuttle's cargo bay, the optical or antenna surface is typically a thin membrane. However, because of the extreme flexibility of both the holding structure and the membrane, the choice of actuators for suppressing the vibration of the membrane causes significant problems. Therefore, this paper studies the use of a passive eddy current damping mechanism to suppress the vibrations of the thin membrane. The damper is of noncontact nature and therefore causes mass loading or additional stiffness, which would change the dynamic response of the structure. Additionally, the noncontact aspect of this system makes its installation extremely easy and ideal for use in space applications.

This manuscript has shown that the ECD can provide significant damping to the extremely thin membranes used in space. Additionally, a theoretical model of an ECD and membrane subjected to an axial load was developed. It was shown through experiments that the model can predict the damping ratio as a function of the gap between the magnet and the conductor with an average accuracy of 8.5% and predict the eigenfrequencies of the system at ambient pressure. The membrane was also tested under vacuum and the damper was demonstrated to reduce the magnitude of the first and third bending modes by 31.06 and 15.62 dB, respectively. However, due to the hygroscopic effects of subjecting the Mylar membrane to vacuum pressure, the material properties and dimensions under vacuum were unable to be determined and the predicted eigenfrequecies became inaccurate. This research has shown the potential of eddy current damping systems for use in space.

Appendix: Solution to Magnetic Flux Density

The integration I_1 in Eq. (10) is

$$I_1 = \int_0^{2\pi} \frac{\sin\phi}{(b^2+z^2-2yb\sin\phi)^{\frac{2}{3}}}\,\mathrm{d}\phi = \frac{1}{bynp^2}\left[m^2\left\{E_1\left(\frac{\pi}{4},\frac{-4yb}{n^2}\right)+E_1\left(\frac{3\pi}{4},\frac{-4yb}{n^2}\right)\right\} - p^2\left\{E_2\left(\frac{\pi}{4},\frac{-4yb}{n^2}\right)+E_2\left(\frac{3\pi}{4},\frac{-4yb}{n^2}\right)\right\}\right] \tag{A1}$$

where

$$m^2 = b^2+y^2+z^2 \tag{A2}$$

$$n^2 = (b-y)^2+z^2 \tag{A3}$$

$$p = (b+y)^2+z^2 \tag{A4}$$

The elliptic integrals of Eq. (A1) are

$$E_1 = (\phi,m) = \int_0^{\phi}(1-m\sin^2\theta)^{\frac{1}{2}}\,\mathrm{d}\theta \tag{A5}$$

$$E_2 = (\phi,m) = \int_0^{\phi}(1-m\sin^2\theta)^{\frac{-1}{2}}\,\mathrm{d}\theta \tag{A6}$$

The integration I_2 in Eq. (11) is

$$I_2 = \int_0^{2\pi} \frac{b-y\sin\phi}{(b^2+z^2-2yb\sin\phi)^{\frac{2}{3}}}\,\mathrm{d}\phi = \frac{1}{bnp^2}\left[s\left\{E_1\left(\frac{\pi}{4},\frac{-4yb}{n^2}\right)+E_1\left(\frac{3\pi}{4},\frac{-4yb}{n^2}\right)\right\} + p^2\left\{E_2\left(\frac{\pi}{4},\frac{-4yb}{n^2}\right)+E_2\left(\frac{3\pi}{4},\frac{-4yb}{n^2}\right)\right\}\right] \tag{A7}$$

where

$$m^2 = b^2+y^2+z^2 \tag{A8}$$

$$n^2 = (b-y)^2+z^2 \tag{A9}$$

$$p = (b+y)^2+z^2 \tag{A10}$$

$$s = b^2-y^2-z^2 \tag{A11}$$

The elliptic integrals of Eq. (A7) are

$$E_1 = (\phi,m) = \int_0^{\phi}(1-m\sin^2\theta)^{\frac{1}{2}}\,\mathrm{d}\theta \tag{A12}$$

$$E_2 = (\phi,m) = \int_0^{\phi}(1-m\sin^2\theta)^{-\frac{1}{2}}\,\mathrm{d}\theta \tag{A13}$$

Acknowledgments

The authors of this paper gratefully acknowledge support from NASA's Graduate Student Researchers Program under Grant NGT-1-03020 from the NASA Langley Research Center and the George R. Goodson Professorship.

References

[1]Grosso, R. P., and Yellin, M., "The Membrane Mirror as an Adaptive Optical Element," *Journal of the Optical Society of America*, Vol. 67, No. 3, 1977, pp. 399–406.

[2]Claflin, E. S., and Bareket, N., "Configuring an Electrostatic Membrane Mirror by Least-Squares Fitting with Analytically Derived Influence Functions," *Journal of the Optical Society of America, A. Optical and Image Science*, Vol. 3, No. 11, 1986, pp. 1833–1839.

[3]Merkle, F., Freischalad, K., and Bille, J., "Development of an Active Optical Mirror for Astronomical Application," *ESO Conference on Scientific Importance of High Angular Resolution at Infrared and Optical Wavelengths*, 1981, pp. 41–52.

[4]Divoux, C., Cugat, O., Basrour, S., Mounaix, P., Kern, P., and Bousse-Saïd, J., "Miniaturized Deformable Magnetic Mirror for Adaptive Optics," *Proceedings of the SPIE Conference on Adaptive Optical System Technologies*, Pt. 2, Vol. 3353, No. 2, 1998, pp. 850–857.

[5]Nelson, G. C., and Main, J. A., "Noncontact Electron Gun Strain Control of Piezoceramics," *AIAA Journal*, Vol. 39, No. 9, 2001, pp. 1808–1813.

[6]Wagner, J., "Optical Metrology of Adaptive Membrane Mirrors," M.S. Thesis, U.S. Air Force Inst. of Technology, Wright–Patterson AFB, OH, March 2000.

[7]Solter, M. J., Horta, L. G., and Panetta, A. D., "A Study of a Prototype Actuator Concepts for Membrane Boundary Control," AIAA Paper 2003-1736, April 2003.

[8]Wiederick, H. H., Gauthier, N., Campbell, D. A., and Rochon, P., "Magnetic Braking: Simple Theory and Experiment," *American Journal of Physics*, Vol. 55, No. 6, 1987, pp. 500–503.

[9]Heald, M. A., "Magnetic Braking: Improved Theory," *American Journal of Physics*, Vol. 56, No. 6, 1988, pp. 521, 522.

[10]Cadwell, L. H., "Magnetic Damping: Analysis of an Eddy Current Brake Using an Airtrack," *American Journal of Physics*, Vol. 64, No. 7, 1996, pp. 917–923.

[11]Lee, K. J., and Park, K. J., "A Contactless Eddy Current Brake System," *Intelligent Processing System, Proceedings, IEEE Conference on Intelligent Processing Systems*, 1998, pp. 193–197.

[12]Genta, G., Delprete, C., Tonoli, A., Rava, E., and Mazzocchetti, L., "Analytical and Experimental Investigation of a Magnetic Radial Passive Damper," *Proceedings of the Third International Symposium on Magnetic Bearings*, 1992, pp. 255–264.

[13]Kligerman, Y., Grushkevich, A., Darlow, M. S., and Zuckerberger, A., "Analysis and Experimental Evaluation of Inherent Instability in Electromagnetic Eddy-Current Dampers Intended for Reducing Lateral Vibration of Rotating Machinery," *Proceedings of ASME, 15th Biennial Conference on Vibration and Noise*, 1995, pp. 1301–1309.

[14]Karnopp, M., "Permanent Magnet Linear Motors Used as Variable Mechanical Damper for Vehicle Suspensions," *Vehicle System Dynamics*, Vol. 18, No. 4, 1989, pp. 187–200.

[15]Schmid, M., and Varga, P., "Analysis of Vibration-Isolating Systems for Scanning Tunneling Microscopes," *Ultramicroscopy*, Vol. 42–44, Pt. B, July 1992, pp. 1610–1615.

[16]Kobayashi, H., and Aida, S., "Development of a Houde Damper Using Magnetic Damping," *Vibration Isolation, Acoustics, and Damping in Mechanical Systems*, Vol. 62, American Society of Mechanical Engineers, 1993, pp. 25–29.

[17]Kienholtz, D. A., Pendleton, S. C., Richards, K. E., and Morgenthaler, D. R., "Demonstration of Solar Array Vibration Suppression," *Proceedings of SPIE's Conference on Smart Structures and Materials*, Vol. 2193, 1994, pp. 59–72.

[18]Kwak, M. K., Lee, M. I., and Heo, S., "Vibration Suppression Using Eddy Current Damper," *Korean Society for Noise and Vibration Engineering*, Vol. 13, No. 10, 2003, pp. 760–766.

[19]Bae, J. S., Kwak, M. K., and Inman, D. J., "Vibration Suppression of Cantilever Beam Using Eddy Current Damper," *Journal of Sound and Vibration*, Vol. 284, Nos. 3–5, 2004, pp. 805–824.

[20]Sodano, H. A., Bae, J. S., Inman, D. J., and Belvin, W. K., "Concept and Model of Eddy Current Damper for Vibration Suppression of a Beam," *Journal of Sound and Vibration*, Vol. 288, 2005, pp. 1177–1196.

[21]Sodano, H. A., Bae, J. S., Inman, D. J., and Belvin, W. K., "Improved Concept and Model of Eddy Current Damper," *Journal of Vibration and Acoustics* (to be published).

[22]Shaker, F. J., "Effect of Axial Load on Modes and Frequencies of Beams," NASA TN D-8109, 1975.

[23]Hall, J., Glease, R. M., and Flint, E., "Dynamic Behavior of Thin Film Membranes," AIAA Paper 2002-1378, April 2002.

[24]Bales, G. L., Hall, J. L., Flint, E. M., and Glease, R. M., "Experimental Issues that Impact In-Vacuum Dynamic Characterization of Thin Film Membranes," AIAA Paper 2003-1743, April 2003.

C. Pierre
Associate Editor